

Does the fine structure constant vary? A third quasar absorption sample consistent with varying α

John K. Webb, Michael T. Murphy, Victor V. Flambaum, Stephen J. Curran

School of Physics, University of New South Wales, Sydney, NSW 2052, Australia

Abstract. We report preliminary results from a third sample of quasar absorption line spectra from the Keck telescope which has been studied to search for any possible variation of the fine structure constant, α . This third sample, which is larger than the sum of the two previously published samples, shows the same effect, and also gives, as do the previous two samples, a significant result. The combined sample yields a highly significant effect, $\Delta\alpha/\alpha = (\alpha_z - \alpha_0)/\alpha_0 = -0.57 \pm 0.10 \times 10^{-5}$, averaged over the redshift range $0.2 < z < 3.7$. We include a brief discussion of small-scale kinematic structure in quasar absorbing clouds. However, kinematics are unlikely to impact significantly on the averaged non-zero $\Delta\alpha/\alpha$ above, and we have so far been unable to identify any systematic effect which can explain it. New measurements of quasar spectra obtained using independent instrumentation and telescopes are required to properly check the Keck results.

Keywords: line: profiles – instrumentation: spectrographs – methods: data analysis – techniques: spectroscopic – quasars: absorption lines

1. Experimental status

Any variation in $\alpha \equiv e^2/\hbar c$ would cause shifts in the relative positions of atomic resonance transitions. Astrophysical measurements permit tests over cosmological time-scales through spectroscopy of high redshift gas clouds seen in absorption against background quasars. Recently we introduced a new method for the analysis of absorption systems seen in optical quasar spectra (the “*many multiplet method*”). This technique provides an order of magnitude increase in precision over the earlier “*alkali doublet*” method for the same quality of data (Webb et al., 1999; Dzuba et al., 1999b).

The many multiplet method compares wavelengths from many species, exploiting the fact that the ground state levels have an enhanced sensitivity, compared to excited levels, to any variation in α .

The dependence of the observed wavenumber, ω_z , on α is most conveniently expressed as $\omega_z = \omega_0 + q \left[\left(\frac{\alpha_z}{\alpha_0} \right)^2 - 1 \right]$. ω_0 is the present-day laboratory wavenumber and ω_z is the wavenumber in the rest-frame of the absorber at the absorption redshift, z . α_0 is the present-day value



© 2018 Kluwer Academic Publishers. Printed in the Netherlands.

of the fine structure constant and α_z is the value at the absorption redshift.

The q coefficients quantify the relativistic correction for a particular atomic mass and electron configuration. These coefficients have been calculated using accurate many-body theory methods (Dzuba et al., 1999b; Dzuba et al., 1999a; Dzuba et al., 2001; Dzuba et al., 2002). The parameterization of ω_z above means that any uncertainties in the numerical values of the q coefficients will not introduce an artificial non-zero value of $\Delta\alpha/\alpha$.

An important characteristic of the many-multiplet method is that a given variation in α produces wavelength shifts for different species which vary greatly in magnitude and which can be in opposite directions. i.e. the q coefficients can be of opposite sign (for the same species in some cases) and vary by up to two orders of magnitude in numerical value (Figure 1). This latter effect can be understood in terms of the atomic orbital properties and the way in which α effects them. This characteristic enhances the power of the many-multiplet because it helps to reduce the impact of any systematic effects in wavelength calibration of the data. Since absorption clouds appear at all redshifts, the observed transitions sample the entire observed wavelength range. It is therefore hard to conceive a systematic error in the wavelength calibration which could emulate the distinctive pattern of shifts caused by a change in α , when a range of different transitions are included in the fit.

In order to exploit the enhanced sensitivity defined by the q values, new high precision laboratory measurements of ω_0 for the species observed were carried out using Fourier transform spectrographs (Pickering et al., 1998; Pickering et al., 2000; Griesmann and Kling, 2000). Several experiments have been completed and new highly precise laboratory wavelengths measured for 16 transitions. The improvement in the accuracy of these wavelengths is 1–2 orders of magnitude compared to the compilation of Morton (1991).

Three independent samples of Keck quasar spectra have now been analysed, covering a broad redshift range. Two of these three samples have been previously published. The first sample (Churchill and Vogt, 2001) used transitions in several Mg II and Fe II multiplets in 30 quasar absorbers. These data provided the first statistically significant effect in the data which was consistent with a variation in α over the redshift range $0.5 < z < 1.6$ (Webb et al., 1999).

A second independent sample, of damped Lyman- α absorbers, (Prochaska and Wolfe, 1999) used *different* atomic transitions (including Ni II, Zn II, Cr II, Al II and Al III) and produced the same statistically significant non-zero result for $\Delta\alpha/\alpha$ over the redshift range $1.8 < z < 3.5$. The

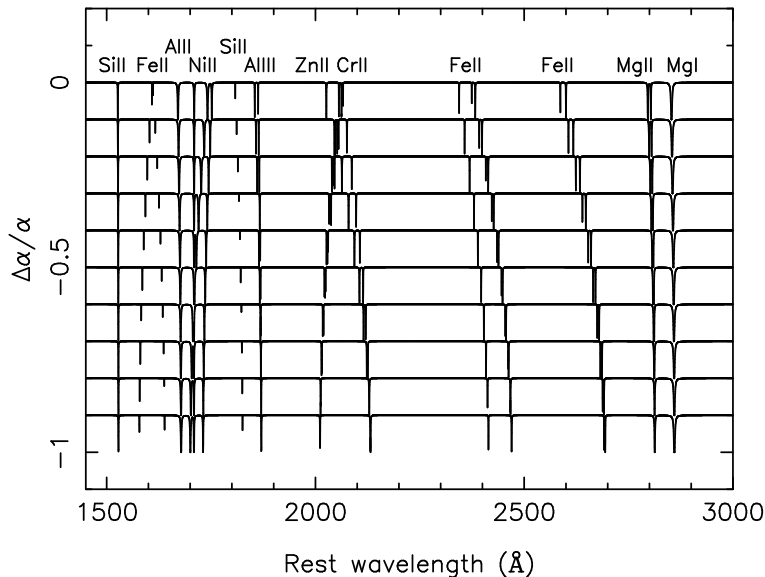


Figure 1. Illustration of line shifts as a function of α for the multiplets used in our analysis. Note how Mg and Si act as “anchor” lines, and how Zn and Cr move in opposite directions.

results of these first 2 samples are summarised in Webb et al. (2001) and full analysis details are given in Murphy et al. (2001a).

The analysis of the third sample (graciously provided by W. Sargent and collaborators) is now complete and we report the preliminary results here. Each of the three samples produces the same result and for the entire dataset, comprising all three samples, the result is $\Delta\alpha/\alpha \equiv (\alpha_z - \alpha_0)/\alpha_0 = (-0.57 \pm 0.10) \times 10^{-5}$ for the redshift range $0.2 < z < 3.7$. We are unable to explain this result in terms of any systematic error despite an exhaustive search (Murphy et al., 2001b).

2. A third independent quasar absorption line sample

The new sample, like the previous two, was also obtained using the HIRES spectrograph on the Keck telescope. The spectral resolution is $\text{FWHM} \approx 6.6 \text{ km s}^{-1}$ and the signal-to-noise ratio per pixel averages 30, with most of the sample in the range 10 to 50. Individual exposure times ranged from 1000 to 6000 s depending on the quasar’s apparent magnitude. Several individual exposures were combined to make the final spectrum. The reader is referred to Murphy et al. (2001b) for specific details regarding the correction of the wavelength scales to vacuum wavelengths.

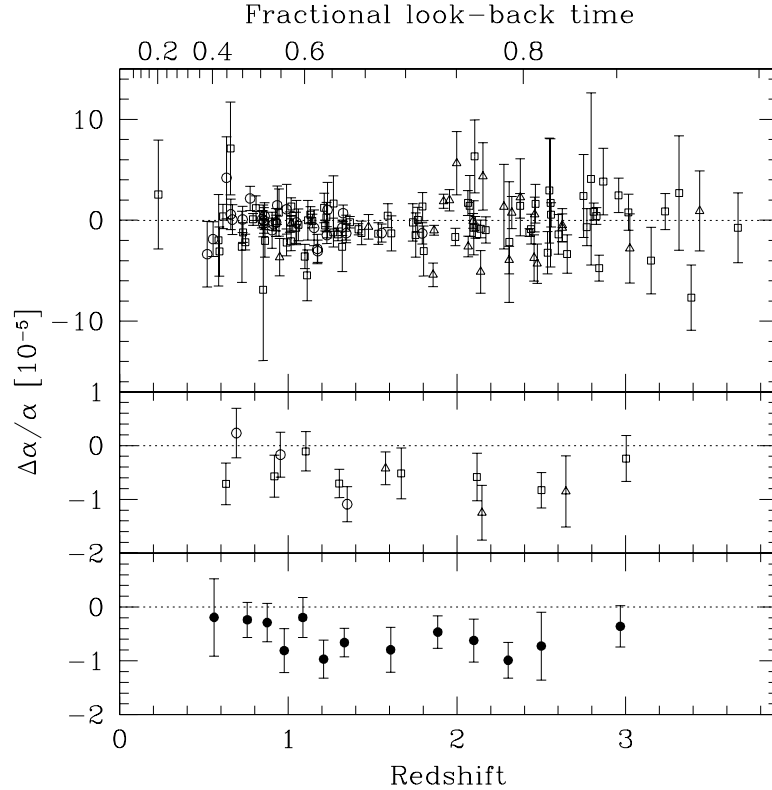


Figure 2. All results from the many-multiplet method to date. $\Delta\alpha/\alpha$ for all 3 samples combined. Hollow circles (Churchill), triangles (Prochaska and Wolfe), squares (Sargent). Upper panel: unbinned individual values. Middle panel: binned but different symbols still reveal results for each sample. Lower panel: binned over the whole sample.

78 absorption systems were identified which contain a sufficiently large sample of transitions such that the many-multiplet method can provide meaningful constraints on $\Delta\alpha/\alpha$. The redshift range covered by this sample is $0.2 < z < 3.7$. As with the previous two samples, this broad redshift coverage means that $\Delta\alpha/\alpha$ is derived using different sets of transitions at different redshifts.

3. Systematic effects and numerical analysis considerations

Here we begin a discussion of systematic effects. The discussion continues in the companion paper in this volume, Murphy et al. (2003).

3.1. WAVELENGTH DISTORTIONS

The simplest systematic problem one can imagine is a low order distortion in the wavelength scale due to errors in the wavelength calibration procedure. Quasar exposures at the telescope are bracketed in time by exposures of a standard calibration source, ThAr. The ThAr laboratory wavelengths are taken from Palmer and Engleman (1983) and Norlén (1973) and the measurement errors in the individual ThAr wavelengths are $\sim 5 \times 10^{-5} \text{Å}$. Assuming no systematic trends, and taking the literature-quoted errors, these errors are too small by a factor of ~ 40 to produce a $\Delta\alpha/\alpha$ at the level we observe.

However, any mistakes made during the process of transferring wavelength information from the ThAr to quasar exposures could in principle emulate a non-zero $\Delta\alpha/\alpha$. To check this, we repeat a test previously applied to samples 1 and 2, analysing the ThAr emission line spectra in the same way as the quasar spectra (Murphy et al., 2001b). For every transition in every quasar absorption system, we identify individual ThAr emission lines in the corresponding calibration spectra which fall close to the observed quasar absorption line wavelengths. These emission lines are then fitted with Gaussian profiles instead of Voigt profiles. We parameterize the “observed” ThAr wavelength using the same relation given in Section 1 in this paper, using the known ThAr laboratory wavelength for ω_0 , but still using the q coefficients from the quasar transition. We then fit the ThAr datasets, which directly sample the same wavelength regions as do the quasar transitions, for all absorption systems in all quasars. In this way, the ThAr spectra become “fake quasar spectra”, and provide a direct test on the reliability of the wavelength calibration procedure.

The results are illustrated in Figure 3. The “ $\Delta\alpha/\alpha$ ” for the ThAr points are plotted on the same scale as the quasar results. This test demonstrates conclusively that the calibration process itself introduces no significant errors.

3.2. MINIMISING THE NUMBER OF FREE PARAMETERS

Although the analysis methods have been applied extensively in other contexts, and have also been described elsewhere in detail as applied to $\Delta\alpha/\alpha$, we re-iterate some of the features of the numerical methods which are of particular importance here. The absorption systems are essentially always found to comprise multiple components, spread over 10s to 100s of kms^{-1} . Two assumptions are made in order to reduce the number of free parameters in the fitting process, and hence to maximise the potential precision of the measurement: (*i*) we adopt the same redshift (as a free parameter) for corresponding components in

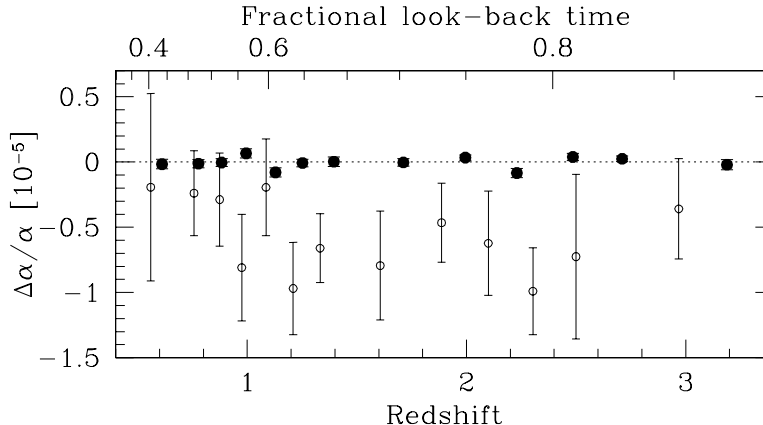


Figure 3. A check on the accuracy of the wavelength calibration. The hollow circles show the binned quasar results. The filled circles show the inferred values using the ThAr calibration spectra as “fake quasar spectra”. Wavelength calibration errors do not produce the signal seen in these quasar data.

different species, (ii) we assume that the line broadening mechanisms for different species are either entirely thermal, or entirely turbulent. Together these amount to the assumption of no spatial or velocity segregation for the species used in estimating $\Delta\alpha/\alpha$.

As a specific example of the reduction in the number of free parameters, one single absorption line from species i (e.g. Mg II 2796Å) is defined by 3 free *cloud* parameters: z_i , b_i , and N_i . z_i is the absorption redshift, b_i is the parameter which describes the atomic velocity dispersion and is related to the rms distribution, v , by $b = \sqrt{2}v$ (kms⁻¹), and N_i is the column density of absorbing atoms (atoms cm⁻²). There are additional *physics* parameters required to describe the line. These include the rest-frame wavenumber of the species, ω_z (determined by $\Delta\alpha/\alpha$ and ω_0 as discussed in Section 1), the oscillator strength and Einstein coefficient for that transition.

If we now include one additional line in the fit (e.g. Fe II 2382Å) then without any assumptions we clearly double the number of free parameters. However, assumptions (i) and (ii) above allow us to reduce this number from 6 to 4 by tying the z ’s and relating the b -parameters by $b_{obs}^2 = b_{thermal}^2 + b_{bulk}^2 = \frac{2kT}{m} + b_{bulk}^2$. In practice, we carry out 2 fits to each absorption system, one at each of the two extreme cases, $T = 0$ (so all species are fitted with the same value of the Doppler parameter, b_{obs}), and $b_{bulk} = 0$ (in which case the b_{obs}^2 for each species are inversely proportional to the atomic mass). We require a consistent solution for $\Delta\alpha/\alpha$ for each fit, otherwise the system is rejected.

A further important technical detail is that the numerical method ensures that the actual constraints on $\Delta\alpha/\alpha$ are derived in a quite natural way from *optically thin* species and not from saturated absorption lines. VPFIT is a non-linear least-squares method. Parameters are estimated using the first and second derivatives of χ^2 with respect to the free parameters. Where multiple components are present, blended in a saturated absorption feature, the value of χ^2 is insensitive to relatively large changes in the component redshifts. Put another way, the derivatives of χ^2 with respect to those redshifts are very small compared to the optically thin case. The consequence of this is that saturated lines contribute little to the overall solution for $\Delta\alpha/\alpha$. This is important to realize because the potential systematic effects due to kinematic cloud structure and possible isotopic abundance evolution may be larger for saturated lines.

We also note that error estimates on $\Delta\alpha/\alpha$ are derived from the diagonal terms of the covariance matrix (inverse of the Hessian matrix) at the best-fit solution. This is a standard technique used in a broad range of applications. The implicit assumption made in ignoring off-diagonal terms is that separate parameters are not closely correlated. This turns out to be a reasonable assumption for $\Delta\alpha/\alpha$ (Figure 1 illustrates why $\Delta\alpha/\alpha$ is not degenerate with redshift). Monte-Carlo methods have also been used to verify this approximation.

Assumptions (i) and (ii) are addressed in the next section.

3.3. THE EFFECT OF CLOUD KINEMATICS AND DYNAMICS ON $\Delta\alpha/\alpha$

For a single absorption system, a non-zero $\Delta\alpha/\alpha$ could be emulated by velocity segregation of the different species observed. This could arise through chemical abundance gradients combined with differential velocity fields. These effects could generate departures from Voigt profiles. However, over an ensemble of random sight-lines, the shifts in $\Delta\alpha/\alpha$ are themselves random, and kinematic effects act just to increase the scatter in a plot such as Fig.2. We now give a brief discussion of the contributory factors to kinematic effects on small velocity scales.

3.3.1. *Small-scale velocity structure*

The large-scale properties of the gas through which the sight-line to the background quasar passes have no influence on estimates of $\Delta\alpha/\alpha$. Galactic rotations or large-scale galactic winds are unimportant. The simple empirical fact that we get excellent agreement between the redshifts of individual components within a quasar absorption complex, down to a small fraction of a kms^{-1} illustrates this. Any contribution

to the scatter in $\Delta\alpha/\alpha$ comes only from the detailed properties of gas on scales smaller than a few kms^{-1} .

Given the importance of small-scale properties in the determination of $\Delta\alpha/\alpha$, it is relevant to ask whether the gas is in equilibrium on these scales, and if not, how the assumption of a Maxwellian atomic velocity distribution inherent in fitting Voigt profiles impacts on $\Delta\alpha/\alpha$ measurements. At the lower redshift end of our sample, a recent detailed study (Churchill, in preparation) suggests that the ratio of the column densities of Mg II and Fe II appears not to change systematically across an absorption complex. A similar chemical uniformity is found for DLAs (Prochaska, 2002). The DLAs show no significant evolution in their number density per unit redshift interval (Rao and Turnshek, 2000). Photo-ionization models applied to the data suggest gas in photo-ionized equilibrium with an ambient extra-galactic background. If this is correct, local equilibrium may be valid, and any redshift evolution of the number of absorption lines per unit redshift interval over and above that expected due to cosmology alone for the Mg II/Fe II absorbers could be explained by cosmological evolution in the integrated background UV flux.

We learn from all the above that there do not seem to be any gross changes in physical conditions over large scales, across an absorption complex. This may imply that we should not expect to find abundance variations and non-equilibrium small-scales.

3.3.2. *Disk and halo models*

In all cases, the $\Delta\alpha/\alpha$ constraints come only from optically thin components. Saturated lines are effectively given zero weight in the parameter estimation procedure as discussed in Section 3.2. From detailed kinematic studies of quasar absorbers (Briggs et al., 1985; Lanzetta and Bowen, 1992; Wolfe and Prochaska, 2000; Churchill and Vogt, 2001), it seems that a disk+halo model provides a reasonable description of the observations. Alternative models exist, including multiple merging clumps bound to dark matter halos (Haehnelt et al., 1998; McDonald and Miralda-Escudé, 1999; Maller et al., 1999) and outflows from supernovae winds (Nulsen et al., 1998; Schaye, 2001).

For disk+halo models of Mg II/Fe II systems, the disk component is generally strongly saturated and spread over small velocity scales. The halo component is more broadly spread in velocity space and causes the lower column density absorption, so the constraints on $\Delta\alpha/\alpha$ from Mg II/Fe II most probably come from the outer parts of galaxy halos. The constraints on $\Delta\alpha/\alpha$ from DLAs arise either from low abundance and hence unsaturated species (e.g. Ni II, Cr II, Zn II), or they come from optically thin components which flank the saturated components (e.g.

Fe II1608 or Al II). We note in passing that any dependence of α on the local gravitational potential could conceivably emulate a cosmological evolution with redshift if DLAs arise in or closer to galaxy disks than the Mg II/Fe II systems.

3.3.3. *Comparison with the ISM*

Analogy with the interstellar medium in our own Galaxy does however suggest that non-equilibrium could apply on very small scales. In an interesting study, Andrews et al. (2001) use stars in a background globular cluster, M92, to probe the kinematics on scales defined by the separation between the lines of sight at the absorber. They find significant variations in Na I column densities in the ISM on scales as small as 1600 AU (or ~ 0.01 pc). Even smaller scale details of the ISM come from measurements of temporal variation of Na I and K I absorption lines, implying non-equilibrium scales $\sim 10 - 100$ AU (Crawford et al., 2000; Lauroesch et al., 2000; Price et al., 2000). These ISM sizes are small compared to estimates of the sizes of individual cloud components, $\sim 10-100$ pc (Churchill and Vogt, 2001). However, it should also be noted that gas densities appear to be quite different and so the comparison should be treated with caution.

3.3.4. *Quasar emission region size and cloud structure*

There may also be important geometric issues. A characteristic size for a quasar continuum emission region may be $\sim 10^{-3}$ pc. The intervening ISM cloudlet “sees” an illuminating source which is thus not quite a perfect point source and the light rays from the edges of the quasar continuum region pass through slightly different regions of space at the absorber. Consider a quasar at $z_{em} = 1$ and an absorber at $z_{abs} = 0.5$. The transverse separation between the light rays at the absorber are only about 25% smaller than the emission region (this is cosmology dependent, but the argument here is illustrative). Thus, the applicability of Voigt profiles, which assume a Maxwellian atomic velocity distribution, depends on the kinematics and dynamics of the ISM in the intervening galaxy on scales of $\sim 10^{-3}$ pc.

3.3.5. *Gravity*

Some theories argue that gravity may be important for cloud confinement on small scales in the Galactic ISM (Walker and Wardle, 1998). If gravity plays a significant role in quasar absorption systems on similar velocity scales, we could apply a simple stability condition, $v^2 = GM/R$ where M and R are the cloudlet mass and radius. Estimates for cloudlet sizes and radii vary but adopting $R = 10$ pc and $M = 30 M_{\odot}$ (Churchill and Vogt, 2001) we get $v \approx 0.1 \text{ kms}^{-1}$. In this case, we get an upper

limit on the velocity shift between different species. For one single Mg II/Fe II absorber, this velocity shift translates into an error on an individual $\Delta\alpha/\alpha$ measurement of roughly half the detected effect. However, this would be randomized over ~ 100 observations, producing a maximum effect which is 20 times smaller than that observed.

3.3.6. Observed scatter in Fig.2

The $\Delta\alpha/\alpha$ points in Fig.2 may give some hint of kinematic effects. At lower redshift, the scatter in the $\Delta\alpha/\alpha$ points is consistent with the statistical error bars, which are derived on the basis of the signal-to-noise ratio and spectral resolution, and assume that the best-fit solution is the correct one. Any particular fit for a set of multiple components to an absorbing complex is not unique. Missing weak components will frequently or perhaps always be present. It is extremely unlikely however that these components can systematically affect $\Delta\alpha/\alpha$ when averaged over a large sample. The effect of missing components will be to increase the random scatter in the individual $\Delta\alpha/\alpha$ values.

At higher redshift, i.e. for the DLAs, this seems to happen to a greater extent than for the lower redshift points. This is to be expected for the following reasons: (a) at higher z (the DLAs), a larger number of different species (e.g. Si II, Fe II, Ni II, Zn II, Cr II) are generally available for fitting compared to lower z (i.e. Mg II and Fe II). The range in optical depths for corresponding velocity components for the DLAs is significantly larger than for the lower z Mg II/Fe II systems. Abundance and ionization variations are therefore likely to be more noticeable. In other words, in general, inter-comparing more species is likely to lead to greater scatter in $\Delta\alpha/\alpha$; (b) if DLAs have a more complex velocity structure, i.e. the number of absorbing components per kms^{-1} may be higher than for the Mg II/Fe II systems, deblending would be more difficult, increasing the uncertainty on $\Delta\alpha/\alpha$; (c) with the DLAs, we have more low- b species compared to Fe II/Mg II. These features are closer to the resolution of the instrument, so there is an increased systematic bias against finding the weaker components.

4. Summary and the next step

We have now analysed three large samples of high quality quasar spectra. All three produce a significant effect in the data which is consistent with varying α . None of the systematic effects so far identified explain the effect. Kinematic effects will be randomized over a large sample such as this, but will contribute to the overall scatter in the individual $\Delta\alpha/\alpha$. The discussion above gives a preliminary guide to the contributory

factors, which need quantifying in detail, in order to fully understand the scatter in the $\Delta\alpha/\alpha$ points over and above pure statistics.

The fact that the higher redshift points exhibit more scatter suggests our precision is close to being limited by systematics. This in turn suggests that further observations of quasar spectra should probably aim at increasing the number of absorption systems studied, rather than increasing the signal-to-noise. However, it is important to study any possible departures from Voigt profiles in detail, and a targeted study at the highest possible signal-to-noise and resolution is important for this goal, for a small number of quasars.

All three samples come from Keck/HIRES. Whilst we have no reason to suspect an instrument-dependent effect, this must obviously be checked. Observations with VLT and Subaru will enable this.

Benefitting from the extra-solar planetary developments, using iodine cells is an obvious way to completely remove any issues concerning the different optical paths taken by quasar and calibration lamp-light, and may eventually provide the acid-test.

Acknowledgements

This work relies on the superb quasar spectroscopic observations of Chris Churchill and collaborators, Art Wolfe and Jason Prochaska, and Wal Sargent and collaborators. The data used in this work corresponds to a mammoth effort on their part and we very gratefully acknowledge their crucial contributions. We also thank John Barrow, Chris Churchill, Joe Wolfe and Frank Briggs for useful discussions. It is a pleasure to thank Graca Rocha and Carlos Martins for organizing the enjoyable conference at which this work was presented, not forgetting Taylors Port for the hangover after the conference dinner. We gratefully acknowledge the John Templeton Foundation for financially supporting this project.

References

- Andrews, S. M., Meyer, D. M. and Lauroesch, J. T.: 2001, *Astrophys. J.* **552**, L73.
 Briggs, F. H., Wolfe, A. M., Turnshek, D. A. and Schaeffer, J.: 1985, *Astrophys. J.* **293**, 387.
 Churchill, C. W. and Vogt, S. S.: 2001, *Astron. J.* **122**, 679.
 Crawford, I. A., Howarth, I. D., Ryder, S. D. and Stathakis, R. A.: 2000, *Mon. Not. Roy. Soc.* **319**, L1.
 Dzuba, V. A., Flambaum, V. V., Kozlov, M. G. and Marchenko, M.: 2002, *Phys. Rev. A* **66**, 022501.

- Dzuba, V. A., Flambaum, V. V., Murphy, M. T. and Webb, J. K.: 2001, *Phys. Rev. A* **63**, 42509.
- Dzuba, V. A., Flambaum, V. V. and Webb, J. K.: 1999a, *Phys. Rev. A* **59**, 230.
- Dzuba, V. A., Flambaum, V. V. and Webb, J. K.: 1999b, *Phys. Rev. Lett.* **82**, 888.
- Griesmann, U. and Kling, R.: 2000, *Astrophys. J.* **536**, L113.
- Haehnelt, M. G., Steinmetz, M. and Rauch, M.: 1998, *Astrophys. J.* **495**, 647.
- Lanzetta, K. M. and Bowen, D. V.: 1992, *Astrophys. J.* **391**, 48.
- Lauroesch, J. T., Meyer, D. M. and Blades, J. C.: 2000, *Astrophys. J.* **543**, L43.
- Maller, A., Somerville, R. S., Prochaska, J. X. and Primack, J. R.: 1999, in: A. J. Bunker and W. J. M. van Breugel (eds.): *The Hy-Redshift Universe: Galaxy Formation and Evolution at High Redshift*, Vol. 193 of *ASP Conf. Ser.*, San Francisco, CA, U.S.A, p. 608.
- McDonald, P. and Miralda-Escudé, J.: 1999, *Astrophys. J.* **519**, 486.
- Morton, D. C.: 1991, *Astrophys. J. Supp.* **77**, 119.
- Murphy, M. T., Webb, J. K., Flambaum, V. V., Churchill, C. W. and Prochaska, J. X.: 2001b, *Mon. Not. Roy. Soc.* **327**, 1223.
- Murphy, M. T., Webb, J. K., Flambaum, V. V. and Curran, S. J.: 2003, in: C. J. A. P. Martins (ed.): *The cosmology of extra dimensions and varying fundamental constants*, Netherlands, Kluwer.
- Murphy, M. T., Webb, J. K., Flambaum, V. V., Dzuba, V. A., Churchill, C. W., Prochaska, J. X., Barrow, J. D. and Wolfe, A. M.: 2001a, *Mon. Not. Roy. Soc.* **327**, 1208.
- Norlén, G.: 1973, *Phys. Scr.* **8**, 249.
- Nulsen, P. E. J., Barcons, X. and Fabian, A. C.: 1998, *Mon. Not. Roy. Soc.* **301**, 168.
- Palmer, B. A. and Engleman, R.: 1983, 'Atlas of the Thorium spectrum'. Technical report, Los Alamos National Laboratory, NM, USA.
- Pickering, J. C., Thorne, A. P., Murray, J. E., Litzén, U., Johansson, S., Zilio, V. and Webb, J. K.: 2000, *Mon. Not. Roy. Soc.* **319**, 163.
- Pickering, J. C., Thorne, A. P. and Webb, J. K.: 1998, *Mon. Not. Roy. Soc.* **300**, 131.
- Price, R. J., Crawford, I. A. and Barlow, M. J.: 2000, *Mon. Not. Roy. Soc.* **312**, L43.
- Prochaska, J. X.: 2002, *Astrophys. J.*, *accepted*. astro-ph/0209193.
- Prochaska, J. X. and Wolfe, A. M.: 1999, *Astrophys. J. Supp.* **121**, 369.
- Rao, S. M. and Turnshek, D. A.: 2000, *Astrophys. J. Supp.* **130**, 1.
- Schaye, J.: 2001, *Astrophys. J.* **559**, L1.
- Walker, M. and Wardle, M.: 1998, *Astrophys. J.* **498**, L125.
- Webb, J. K., Flambaum, V. V., Churchill, C. W., Drinkwater, M. J. and Barrow, J. D.: 1999, *Phys. Rev. Lett.* **82**, 884.
- Webb, J. K., Murphy, M. T., Flambaum, V. V., Dzuba, V. A., Barrow, J. D., Churchill, C. W., Prochaska, J. X. and Wolfe, A. M.: 2001, *Phys. Rev. Lett.* **87**, 091301.
- Wolfe, A. M. and Prochaska, J. X.: 2000, *Astrophys. J.* **545**, 603.